2013 21st Mediterranean Conference on Control & Automation (MED)
Platanias-Chania, Crete, Greece, June 25-28, 2013

EMG based classification of basic hand movements based on time-frequency features

Christos Sapsanis, George Georgoulas and Anthony Tzes, *Senior Member, IEEE*

***Abstract*—This paper proposes an integrated approach for the identification of daily hand movements with a view to control prosthetic members. The raw EMG signal is decomposed into Intrinsic Mode Functions (IMFs) with the use of Empirical Mode Decomposition (EMD). A number of features are extracted in time and in frequency domain. Two different dimentionality methods are tested, namely the Principal Component Analysis (PCA) technique and the RELIEF feature selection algorithm. The outputs of the dimensionality reduction stage are then fed to a linear classifier to perform the detection task. The approach was tested on a group of young individuals and the results appear promising.**

***Index Terms*—Biomedical signal analysis, Empirical Mode Decomposition, RELIEF feature selection. Principal Component analysis, pattern classification, electromyography.**

I. Introduction

Biosignals [1] refer to collective electrical signals acquired from any organ that represents a physical variable of interest. The nervous system controls the muscles' contraction and relaxation. The signal acquired from muscles can be detected using biosensors [2]. Electromyogram (EMG) signal is the biosignal that measures the activity produced by skeletal muscles during their contraction representing neuromuscular activities. The EMG signal of a specific muscle is quite noisy due to the contribution of the surrounding muscles and usually requires a series of pre-processing steps before becoming suitable for further processing.

EMG-signal seems to be a viable candidate for the hand's movement classification due to the distinct signature of each movement on the produced signal. In the field of biomechatronics, the use of EMG-signals as an input in decision making systems is a vital part in order to control effectively a robotic exoskeleton (hand, arm and lower limbs) [3]. In addition, it has been used also for recreational activities and especially for video games [4]. The turning point in using EMG is the fact that it is more comfortable for a hand amputee to wear a glove that includes the EMG electrodes rather than using the promising electro-encephalography (EEG) electrodes in the area of the head [5].

C. Sapsanis and A. Tzes are with the Department of Electrical and Computer Engineering, University of Patras, Greece, e-mail: csapsanis@ieee.org, tzes@ece.upatras.gr).

G. Georgoulas is with KIC Laboratory, Department of Informatics and Telecommunications Technology, Technological Educational Institute of Epirus, GR-47100, Greece, e-mail: georgoul@teleinfom.teiep.gr

Solving the motion command identification problem using EMG signals has been investigated from several research groups with low classification error, at the expense of using many (more than 4) electrodes [6]. Using such a large number of electrodes can be an obstacle for the creation of a system friendly to the patient and inexpensive from a financial point of view. Furthermore, most commercial dexterous prosthetic systems allow the amputee to command a grasp posture and force just by performing the corresponding action with the exoskeleton prosthetic hand using no more than two electrodes [7].

This paper tackles the identification of basic hand movements using surface-EMG-data based on an advanced signal processing techniques. The EMG signals were acquired using two electrodes attached on two specific muscles of the hand. Our previous work [8] has indicated that the use of Empirical Mode Decomposition (EMD) can enhance the identification accuracy of a pattern recognition scheme. In this work we further exploit the use of EMD, extracting features in the frequency domain, while inserting a dimensionality reduction stage which is based either on Principal Component Analysis or RELIEF feature selection algorithm, before the application of the classifier. Our results show that the information carried by the EMD extracted features in the frequency domain, can further increase the classification accuracy [8], whereas the results of dimensionality reduction stage suggests that the features carry complementary information. The rest of this paper is structured as follows. Section II describes the experimental setup and the classification technique. The experimental results are highlighted in Section III and concluding remarks appear in Section IV.

II. EMG-Data Based Hand Movement Classification

The problem of hand movement identification is cast as a typical supervised pattern recognition problem. Based on a collected set of raw EMG-recordings, a preprocessing stage excludes the non-contracting portions at the beginning of each movement. Following the muscle contraction detection, segmentation of the rest of the signal takes place using overlapping time-windows. From each segment a number of features is extracted using both the signal as well as its Intrinsic Mode Functions (IMFs) computed after the application of EMD. Due to the high dimensionality of the produced feature vector, two methods for dimensionality reduction were tested before the application of a simple linear classifier which attempts to classify each segment to one of the six basic hand movements described in the next section.

A. EMG Data Collection

The experiments consisted of freely and repeatedly grasping of different items which were essential to conduct the hand movements. The speed and force were intentionally left to the subject's will. There were 2 forearm surface EMG electrodes Flexor Capri Ulnaris and Extensor Capri Radialis, Longus and Brevis [9]) held in place by elastic bands and the reference electrode in the middle, in order to gather information about the muscle activation.

For the data collection six healthy subjects (2 males and 4 females) of the same age approximately (20 to 22-year-old) were asked to repeat the following six movements (Figure 1): a) Spherical (S): for holding spherical tools, b) Tip (T): for holding small tools, c) Palmar (P): for grasping with palm facing the object, d) Lateral (L): for holding thin, flat objects, e) Cylindrical (C): for holding cylindrical tools and f) Hook (H): for supporting a heavy load. For each movement the subject was asked to perform it for 6 seconds and the whole procedure was repeated 30 times for each basic movement. Therefore for each subject a total of 180 6-second long 2-channel EMG signals were recorded.

The data were collected at a sampling rate of 500 Hz, using as a programming kernel the National Instrument's (NI) Labview [10]. The signals were band-pass filtered using a Butterworth Band Pass filter with low and high cutoff 15Hz and 500Hz respectively and a notch filter at 50Hz to eliminate line interference artifacts.

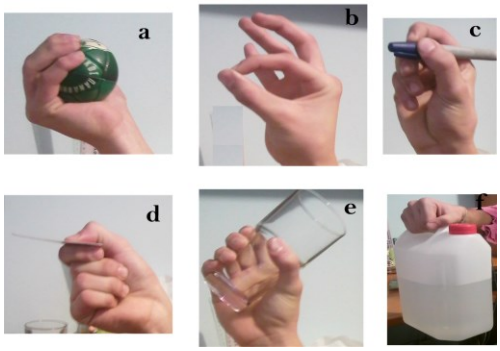

Figure 1. Illustration of the hand gestures.

The hardware that was used (Figure 2) was an analog/digital conversion card NI USB-6009, mounted on a PC. The signal was acquired from two Differential EMG Sensors and the signals were transmitted to a 2-channel EMG system by Delsys Bagnoli™ Handheld EMG Systems [11].

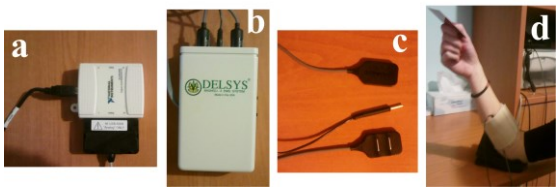

Figure 2. The experimental setup. a) National Instruments analog/digital conversion card, b) 2-channel EMG system, c) 2 Differential and 1 reference EMG Sensor and d) the setup applied on a subject.

B. *Preprocessing*

The sliding time-window approach [12] was applied, with a view to focus only on segments where the muscle is contracted. Within a sliding window of 40 ms the average IEMG value (see section II.D) was calculated. Once that value exceeded a predefined threshold (set equal to 10 in this study) we considered that the muscle was no longer in a resting phase and we started processing the rest of the recording. A characteristic pattern of the increase of the IEMG value as a subject moves from rest mode to contraction mode is depicted in Figure 3. As it can be seen once the contraction is initiated a high value of IEMG is reached which afterwards settles to a lower level, fluctuating around it.

Rather than using an adjacent data windowing, the overlapping windowing [12] approach was employed in this work, with time windows of 300 ms and a time leap of 30 ms (Figure 4). In each segment we applied EMD for the extraction of IMFs.

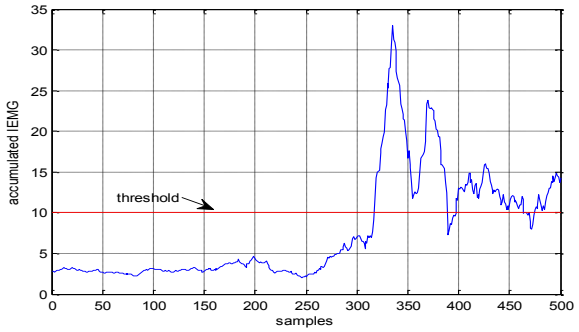

Figure 3. Illustration of evolution of the accumulated IEMG values moving from a resting phase to full muscle contraction, along with the predefined threshold; based on the threshold, the muscle is contracted at the 320th sample.

C. *Empirical Mode Decomposition*

Since the hand-gestures are considered as non-linear and non-stationary processes, decomposition algorithms that assume linearity and stationarity might provide misleading results. EMD [13] is a quite new adaptive method for analyzing non-linear and/or non-stationary signals, and has been applied in a variety of areas.

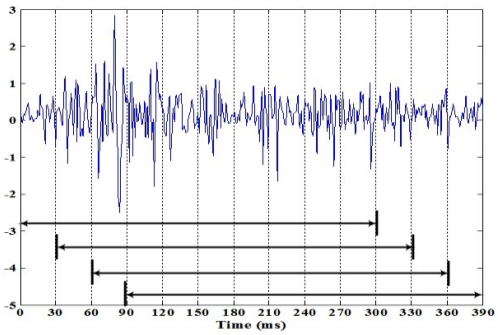

Figure 4. 300 msec long overlaping windows

Given a signal $x(t)$ the EMD algorithm decomposes the signal into a number of IMFs using the following procedure:

1. All the local minima and local maxima of $x(t)$ are located and used to create an upper ($e_{max}(t)$) and a lower ($e_{min}(t)$) envelope through interpolation (usually via cubic interpolation)
2. The running mean is calculated using the envelopes extracted in step 1 $m(t) = \left(e_{\min}(t) + e_{\max}(t)\right)/2$
3. The running mean is subtracted from the signal and what is left is called the detail signal $d(t)=x(t)-m(t)$.
4. The whole process is repeated by replacing $x(t)$ with $m(t)$ until the final residual is a monotonic function (or a user specific number of IMFs has been extracted– application dependant).

In practice, step 3 may not produce a valid IMF. As a result, sifting needs to take place, upon the detail $d(t)$ until a specific criterion is met [13], [14]. Therefore, the original signal $x(t)$ is eventually decomposed into a sum of IMFs plus a residual term: $x(t) = \sum_i IMF_i(t) + r(t)$.

Following the implementation of the EMD algorithm, the Hilbert transform can be applied to each IMF separately and then the instantaneous frequency can be calculated as the derivative of the phase function.

After performing the Hilbert transform [15] to each IMF the original signal can be expressed as the real part (RP), in the following form

$$x(t) = RP\left(\sum_j a_j(t)e^{i\theta_j(t)}\right) = RP\left(\sum_j a_j(t)e^{i\int\omega_j(t)dt}\right) \qquad (1)$$

The amplitude and frequency of each component as a function of time, can thus be found from (1). This time-frequency distribution of the amplitude is called the Hilbert-Huang spectrum ($H(\omega,t)$).

Figure 5 and 6 depict one of the two EMG signals along with the corresponding first three IMFs for the case of: a) Hook movement and b) Spherical movement, while Figures 7 and 8 depict the respective Hilbert-Huang representations.

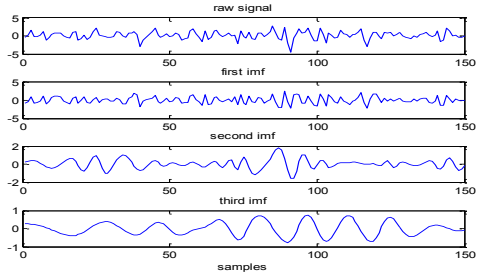

Figure 5. Raw EMG signal and first 3 IMFs for Hook movement

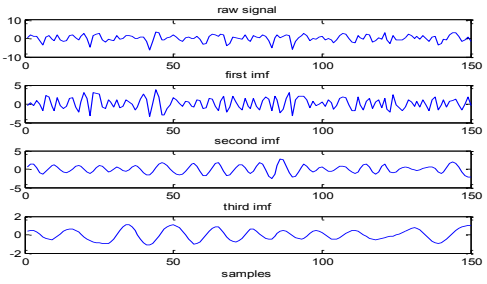

Figure 6. Raw EMG signal and first 3 IMFs for Spherical movement

D. *Feature extraction*

Raw signals are rarely involved in pattern recognition applications. A feature extraction stage is usually involved in order to condense the relevant information and also alleviate the problem due to the curse of dimensionality. The features should be selected in such a way as to maximally separate the desired output classes.

In [8], eight popular features (Integrated Electromyogram (IEMG), zero-crossing, Slope Sign Changes, waveform length, Willison amplitude, variance, skewness and kurtosis) [16] were extracted, not only from the original EMG signals but from the three IMFs that were produced after processing the EMG signals with the help of EMD toolbox [17] as well as from the residual.

In this work apart from the aforementioned features (per EMG channel and per IMF) the median, the standard deviation and the kurtosis of the instantaneous frequencies (IFs) of the three IMFs were also included in the feature vector. As it can be seen in figures 9 and 10, where the median of the IF of the first two IMFs are depicted, some of the movements can have a distinct pattern in the frequency domain too. For the specific subject (#1). the cylindrical movement can be separated from the spherical using the frequency information of the first IMF, whereas the hook movement can be separated by the spherical using the frequency information coming from the second IMF.

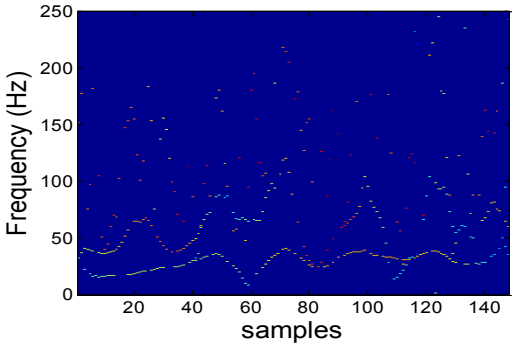

Figure 7. $H(\omega,t)$ corresponding to the Hook-movement IMFs

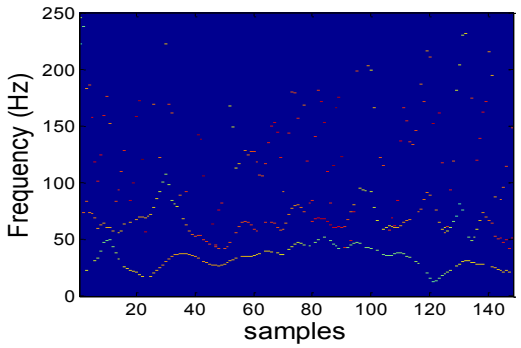

Figure 8. $H(\omega,t)$ corresponding to the Spherical-movement IMFs

A brief description of each feature is given below:

1) Integrated Electromyogram (IEMG):

IEMG is the average value of the absolute values of EMG: $IEMG = \frac{1}{N}\sum_{k=1}^{N}|x_k|$

where x_k is the k[th] sample data out of N samples of EMG raw data.

2) Zero Crossing (ZC):

ZC counts the times that the signal changes sign. Given two contiguous EMG amplitude samples x_k and x_{k+1} the ZC can he calculated as: $ZC = \sum f(x)$, where

$$f(x) = \begin{cases} 1, \ if, (x_k > 0 \ AND \ x_{k+1} < 0) \\ \quad OR \ (x_k < 0 \ AND \ x_{k+1} > 0) \\ 0, \ otherwise \end{cases}, \ k = 1, 2, \ldots, N\text{-}1$$

3) Slope Sign Changes (SSC):

SSC counts the times the slope of the signal changes sign. Given three contiguous EMG amplitude samples x_{k-1}, x_k and x_{k+1}, the number of slope sign changes is given by: $SSC = \sum f(x)$, where

$$f(x) = \begin{cases} 1, \ if, (x_k < x_{k+1} \ AND \ x_k < x_{k-1}) \\ \quad OR \ (x_k > x_{k+1} \ AND \ x_k > x_{k-1}) \\ 0, \ otherwise \end{cases}, \ k = 1, \ldots, N\text{-}1$$

4) Waveform Length (WL):

WL is a cumulative variation of the EMG that can indicate the degree of variation about the EMG signal. It is given by: $WL = \sum_{k=1}^{N-1}(|x_{k+1} - x_k|)$

5) Willison Amplitude (WAMP):

WAMP is the number of counts for each change of the EMG signal amplitude between two adjacent samples that exceeds a defined threshold. It is given by $WAMP = \sum_{k=1}^{N-1} f(|x_{k+1} - x_k|)$

$$f(x) = \begin{cases} 1, & if \ x > threshold \\ 0, & otherwise \end{cases}$$

6) Variance (VAR):

VAR is a measure of the power density of the EMG signal which is given by: $VAR = \frac{1}{N-1}\sum_{k=1}^{N} {x_k}^2$

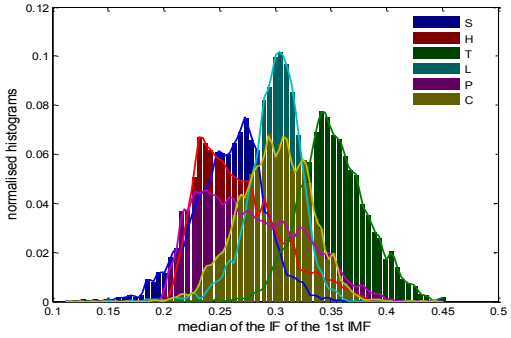

Figure 9. Normalised Histograms ("empirical pdfs") of the median of the IF of the first IMF.

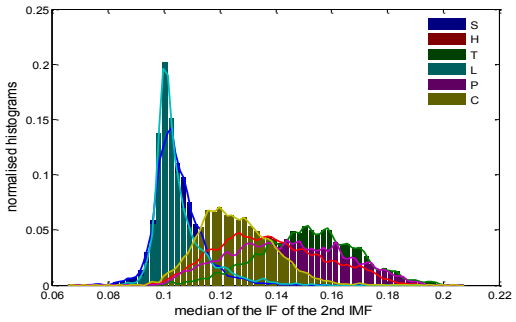

Figure 10. Normalised Histograms ("empirical pdfs") of the median of the IF of the second IMF

7) Skewness

The skewness of a distribution is given by: $s = \frac{E(x-\mu)^3}{\sigma^3}$

8) Kurtosis

The kurtosis of a distribution is given by: $k = \frac{E(x-\mu)^4}{\sigma^4}$

where μ is the mean of x, σ is the standard deviation of x, and $E(x)$ represents the expected value of x.

9) Median

If the count is odd, median is the middle number in a given sequence of numbers but if it is even, median is the average of the two middle numbers.

10) Standard Deviation

The standard deviation (σ) is the square root of the variance

E. Dimensionality reduction framework

Since: a) some of the extracted features can be correlated, therefore conveying redundant information, and b) certain features might be irrelevant and can affect the discriminative capability of the classifier, a dimensionality reduction scheme is usually sought.

There are two major families of dimensionality reduction techniques. The first one maps the original space into a lower dimensional space through a mathematical transformation whereas the second one attempts to select a subset of the original features. In this work we tested two methods for

dimensionality reduction, one from each family of methods: PCA [18] and a filter based feature selection approach using RELIEF [19].

1) Principal Component Analysis

PCA or the Karhunen-Loeve transformation has been used extensively for feature generation and dimensionality reduction in pattern recognition [18]. PCA linearly transforms the original space by projecting the *d*-dimensional data onto the l ($l \leq d$) eigenvectors of their covariance matrix corresponding to the l larger eigenvalues. Even if the entire set of the eigenvectors is to be retained (resulting in a lack of dimensionality reduction) this may still lead to an improvement of classification performance due to the uncorrelated nature of the new set of features.

2) Feature Selection based on the RELIEF algorithm

The successfulness of Relief algorithm is based on its simple and effective evaluation of the features' quality. It is a feature weight based algorithm inspired by instance-based learning [19].

The Relief algorithm searches for the features that are statistically relevant to the target concept using training data *D*, a sample size *m* and a τ-threshold ($\tau \in [0,1]$). The case where the two instances are different can be illustrated with a *diff*-function which takes as input the two instances *X, Y*.
The *diff*-function in the case or numerical (integer or real) is:

$$diff(xk, yk) = (xk - yk)/no\mathrm{k}$$

where no_k is a number used for normalization of the values that are differed in the margins of 0 to 1.
This algorithm selects a sample which is formatted in *m* triplets (*X*, Near-hit, Near-Lose). For the selection of the two last instances, the weight update uses the Euclidean distance. The selected features are the ones that score higher than a user defined threshold.

Relief Algorithm

1st step Separate D into positive (D^+) and negative (D^-) instances
W=(0, 0, …, 0)
2nd step For i=1 to m
Select an instance $X \in D$ randomly
Select one $Z^+ \in D^+$ closest to X randomly
Select one $Z^- \in D^-$ closest to X randomly
if (X is a positive instance)
then Near-hit= Z^+; Near-miss= Z^-
else Near-hit= Z^-; Near-miss= Z^+
For i=1 to p ;the update of the weights
$w_i = w_i - diff(x_i, \text{near-hit}_i)^2 + diff(x_i, \text{near-miss}_i)^2$
3rd step Relevance=.(1/m)W
For i=1 to p
If ($\text{relevance}_i \geq t$)
Then f_i is a relevant feature
Else f_i is a irrelevant feature

The previous formulation applies for the case of binary classification problems. In our case we employed the extension to multiclass problems, called RELIEF-E where the near miss of an instance X is estimated using the nearest neighbor belonging to any other class [20].

F. Classification

After the dimensionality reduction stage the reduced input vector was fed to a linear classifier [21]. Each feature vector $\mathbf{x}$ is assigned to class i for which the value of the corresponding discriminant function is maximum, or

$$i = \arg\max_i \left\{ 2\ln P(\omega_i) - (\mathbf{x} - \boldsymbol{\mu}_i)^T \mathbf{C}^{-1} (\mathbf{x} - \boldsymbol{\mu}_i) \right\},$$

where $\boldsymbol{\mu}_i$ is the mean of class i, $P(\omega_i)$ is the prior probability of class i, and $\mathbf{C}$ is the estimated covariance matrix assumed common for all classes.

III. Experimental Studies

Since the selection of: a) the retained Principal Components (PCs) and/or b) the included features, requires a tuning process and in order to decouple that from the performance estimation an "inner" and an "outer" loop validation scheme was employed. The outer loop was included to assess the performance of our approach while the inner scheme was applied to tune our procedure (number of retained PCs or number of retained features). In the "outer" scheme each time we randomly selected 15 of the recordings for training and the remaining 15 for testing for each one of the 6 movements (at a later step we swapped them - the training set switched to the testing set and vice versa). Following the latter the training set was again divided into training and testing sets (70% for training and 30% for testing). This inner loop was repeated 10 times and the best configuration (number of PCs) or number of features (we did not make use of the threshold parameter and we rather tested all possible numbers (1-96) of retained features), in terms of average classification performance was selected and the model was retrained using both the training and testing sets of the inner loop and validated using the testing set of the outer loop. Hence, the parameter selection stage is decoupled from the estimation of the performance [22] thus avoiding overly optimistic (overfitting) conclusions about the capabilities of our approach. Lastly, the outer loop procedure was repeated 5 times (therefore practically we implemented a 5x2 CV (cross-validation) approach [22]). The results are summarized in Figures 11 and 12 and the aggregated confusion matrices corresponding to the PCA dimensionality reduction are presented in the Appendix.

Due to space limitations the aggregated matrices corresponding to the RELIEF dimensionality reduction stage were not included. However their structure is similar to their PCA counterparts revealing similar misclassification behavior as it can be drawn from Figures 11 and 12 (where no statistically significant differences (significance level a=0.05) were observed between the two dimensionality reduction methods using Wilcoxon's Signed-Rank test [23]).

In most of the cases more than 90 PCs were retained and more than 90 features with the exception of subject #3 which exhibited a trend for retaining ~85 PCs and features. In all cases there is no clear superiority of one method over the

other. Therefore it seems that the features carry complementary information. Moreover the inclusion of the frequency related features resulted in an increase of the overall accuracy of 0.5-1% except again from the case of subject #3 where the results remain at the same level.

The confusion matrices also reveal that almost in all subjects there is an increased mixing between T-L and P movements and S and C (with the exception of subject #1 for both cases and subject # 5 for the case of assigning C movements) but also that each subject exhibits its own peculiarities.

IV. Conclusions

In this work we extended our previous work on the use of EMD for the task of hand movement classification using EMG signals. The included information in the frequency domain further increases the classification accuracy of our method indicating that the constructed feature bank is probably adequate for the problem at hand. On the other hand the variations in the behavior of the classifier among the different subjects reveal the need for fine-tuning of the algorithms for specific misclassifications taking place for each individual.

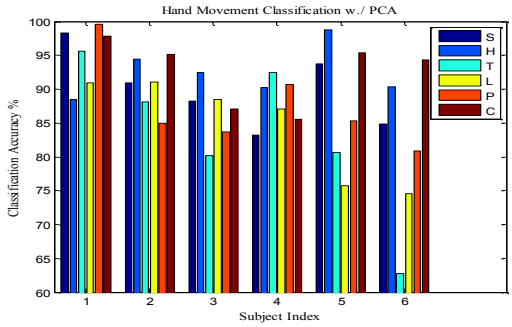

Figure 11. Hand movement classification performance using PCA

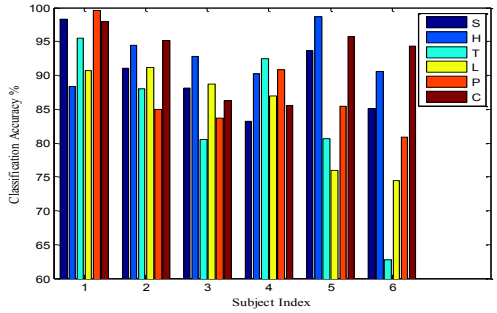

Figure 12. Hand movement classification performance using the Relief Algorithm

Therefore, apart from the use of robust yet simple classifiers such as the one involved in the present study, more advanced algorithms that can focus on the specific misclassifications for each individual, such as error correction code methods, Adaboost etc., will be tested in future work using also a larger database that we are forming involving more subjects. Moreover, the sequential nature of the phenomenon will be taken into account to avoid spurious misclassification by incorporating specific limitations in the transition from one hand movement to another.

Appendix

TABLE I. Aggregated Confusion Matrix Subject #1 w./ PCA

		Predicted					
		S	***H***	***T***	***L***	***P***	***C***
True	***S***	21289	0	0	1	276	89
	H	51	19431	1	1427	0	1055
	T	50	149	18182	224	132	283
	L	0	1355	198	17152	86	74
	P	73	0	1	0	21579	17
	C	124	237	76	12	3	20398

Aggregated Confusion Matrix Subject #2 w./ PCA

		Predicted					
		S	***H***	***T***	***L***	***P***	***C***
True	***S***	17826	130	371	51	54	1163
	H	539	21449	46	602	1	63
	T	3	0	16637	1337	825	93
	L	0	44	1017	16985	588	11
	P	0	0	1898	896	15866	0
	C	597	0	268	31	15	18049

TABLE II. Aggregated Confusion Matrix Subject #3 w./ PCA

		Predicted					
		S	***H***	***T***	***L***	***P***	***C***
True	***S***	18371	673	68	14	13	1701
	H	506	19615	160	59	279	596
	T	0	76	15999	1751	1759	345
	L	0	0	1546	17114	685	0
	P	28	245	1630	1113	16800	254
	C	850	1124	432	54	199	17896

TABLE III. Aggregated Confusion Matrix Subject #4 w./ PCA

		Predicted					
		S	***H***	***T***	***L***	***P***	***C***
True	***S***	18295	1052	2	0	23	2628
	H	1252	19666	61	0	4	817
	T	0	1	17472	276	1116	0
	L	0	0	264	16194	2142	0
	P	0	0	861	882	17052	0
	C	3031	192	0	0	19	19233

TABLE IV. AGGREGATED CONFUSION MATRIX SUBJECT #5 W./ PCA

		Predicted					
		S	***H***	***T***	***L***	***P***	***C***
True	***S***	20149	224	0	0	0	1107
	H	200	21818	0	0	43	24
	T	0	0	14990	2785	825	0
	L	0	0	2141	14092	2367	0
	P	0	4	774	2013	16643	66
	S	413	56	3	0	508	20465

TABLE V. AGGREGATED CONFUSION MATRIX SUBJECT #6 W./ PCA

		Predicted					
		S	***H***	***T***	***L***	***P***	***C***
True	***S***	18912	415	71	630	100	2137
	H	238	19451	0	3	45	1793
	T	169	0	12305	5002	2038	66
	L	112	53	3453	14771	1411	0
	P	7	0	1407	875	15788	1433
	S	372	299	11	16	506	19896

REFERENCES

[1] E. Kaniusas. "Fundamentals of Biosignals" Biomedical Signals and Sensors I, pp. 1-26, 2012.

[2] D. Carroll, A. Subbiah, "Recent Advances in Biosensors and Biosensing Protocols" Journal of Biosensors & Bioelectronics 2012.

[3] K. Andrianesis, A. Tzes, "Design of an anthropomorphic prosthetic hand driven by Shape Memory Alloy actuators" IEEE/RAS-EMBS International Conference on Biomedical Robotics and Biomechatronics, Arizona, USA, pp 517-522, 2008.

[4] T. S. Saponas, D. S. Tan, D. Morris, R. Balakrishnan, J. Turner, J A. Landay "Enabling Always-Available Input with Muscle-Computer Interfaces" in 22nd annual ACM symposium on User interface software and technology, Association for Computing Machinery, New York, USA, pp 167-176, 2009

[5] K. Kiguchi, and Y. Hayashi, "A study of EMG and EEG during perception-assist with an upper-limb power-assist robot" International Conference on Robotics and Automation, Minnesota, USA, pp. 2711 – 271, 2012.

[6] M. A. Oskoei, and H. Hu. "Myoelectric control systems-A survey." Biomedical Signal Processing and Control, vol. 2, no. 4, pp.275-294, 2007.

[7] C. Castellini, E Gruppioni, A Davalli, and G Sandini. "Fine detection of grasp force and posture by amputees via surface electromyography" in Journal of Physiology, pp. 255-62, Sep-Dec 2009.

[8] C. Sapsanis, G. Georgoulas, A. Tzes, "Improving EMG based Classification of basic hand movements using EMD" in 35th Annual International Conference of the IEEE Engineering in Medicine and Biology Society '13, Osaka, Japan, July 2013

[9] E. F. Delagi, A. O. Perotto, J. Iazzetti, and D. Morrison, Anatomical guide for the Electromyographer: The Limbs and Trunk, Charles C Thomas Pub Ltd, 5th ed., 2011.

[10] http://www.ni.com/labview/

[11] http://www.delsys.com/products/bagnoli_handheld.html

[12] H. P. Huang, and C. Y. Chiang. "DSP-based controller for a multi-degree prosthetic hand." Robotics and Automation, 2000. In International Conference on Robotics and Automation'00.. vol. 2, pp. 1378-1383, 2000.

[13] N. E. Huang, Z. Shen, S. R. Long, M. L.Wu, H. H. Shih, Q. Zheng, N. C. Yen, C. C. Tung, and H. H. Liu, "The empirical mode decomposition and Hilbert spectrum for nonlinear and non-stationary time series analysis," in *Proc. of the Royal Society London A*, vol. 454, pp. 903–995, 1998.

[14] G. Rilling, P. Flandrin, and P. Gonçalvès, "On empirical mode decomposition and its algorithms" in *Proc. of 6th IEEE-EURASIP Workshop on Nonlinear Signal and Image Processing* (NSIP '03), Grado, Italy, June 2003.

[15] N. E. Huang and S. S. P. Shen, Hilbert-Huang Tranform and its Applications, World Scientific Publishing Co. Pte Ltd, 2005.

[16] D. Joshi, K. Kandpal, and S. Anand. "Feature evaluation to reduce false triggering in threshold based emg prosthetic hand." International Conference on Biomedical Engineering, pp. 769-772, 2008.

[17] The EMD toolbox <http://perso.ens-lyon.fr/patrick.flandrin/emd.html>

[18] S. Theodoridis, and K. Koutroumbas, Pattern Recognition. 4th ed. Burlington, MA: Academic Press, 2009.

[19] K. Kira and L.A. Rendell, "The Feature Selection Problem: Traditional Methods and a New Algorithm," Proc. 10th Nat'l Conf. Artificial Intelligence, pp. 129-134, 1992.

[20] I. Kononenko, "Estimating attributes: analysis and extensions of RELIEF". In Machine Learning: ECML-94 pp. 171-182, 1994.

[21] D. J. Hand, "Classifier technology and the illusion of progress," Statistical Science, vol. 21, no. 1, pp. 1-14, 2006

[22] L. Salzberg, "On comparing classifiers: Pitfalls to avoid and a recommended approach," Data Mining and Knowledge Discovery, vol. 1, no. 3, pp. 317-328, 1997

[23] N. Japkowicz, M. Shah, Evaluating Learning Algorithms; A Classification Perspective, Cambridge University Press, (2011).